Available online at www.sciencedirect.com
ScienceDirect
Journal of Molecular Catalysis A: Chemical 278 (2007) 112–119
JOURNAL OF MOLECULAR CATALYSIS A: CHEMICAL
www.elsevier.com/locate/molcata

Catalytic properties of Ru nanoparticles introduced in a matrix of hypercrosslinked polystyrene toward the low-temperature oxidation of D-glucose

Esther Sulman [a], Valentine Doluda [a,*], Stanislaw Dzwigaj [b], Eric Marceau [b], Leonid Kustov [c], Olga Tkachenko [c], Alexey Bykov [a], Valentina Matveeva [a], Mikhail Sulman [a], Natalia Lakina [a]

[a] *Tver State Technical University, Department of Biotechnology and Chemistry, Nab. A. Nikitina 22, 170026 Tver, Russia*
[b] *Laboratoire de Réactivité de Surface, Université Pierre et Marie Curie, Paris 6, 4 place Jussieu, 75252 Paris Cedex 05, France*
[c] *Institute of Organic Chemistry by N.D. Zelinsky, Laboratory of Development and Investigation of Polyfunctional Catalysts, Leninsky Prospect 47, Moscow, Russia*

Received 16 May 2007; received in revised form 21 August 2007; accepted 22 August 2007
Available online 2 September 2007

Abstract

The catalytic properties and structural characterization of catalysts derived from hypercrosslinked polystyrene (HPS), a polymer exhibiting mesoporosity and loaded with ruthenium in various amounts are investigated in the oxidation of D-glucose to D-gluconic acid. Transmission electron microscopy, X-ray fluorescence analysis, nitrogen physisorption measurements, diffuse reflectance infrared Fourier transform spectroscopy of adsorbed CO, EXAFS, XANES and catalytic studies show the presence of catalytically active nanoparticles of mixed composition (metal/oxide) with a mean diameter of 1.0–1.2 nm. The most active catalyst is found to contain 0.74 Ru wt.%. The highest selectivity to D-gluconic acid is 99.8% for a conversion of D-glucose of 99%; the specific activity of the catalyst is measured to be 1.13×10^{-3} mol mol^{-1} Ru s^{-1}. The high-catalytic activity is attributed to the presence of pores of various sizes which facilitate mass transport and the high stability is attributed to the presence of small mesopores that have high-sorptional capacity and hinder the migration of the nanoparticles.

Keywords: D-Glucose; Oxidation; Ruthenium; Nanoparticles; Hypercrosslinked polystyrene

1. Introduction

In recent years, catalysts containing metal nanoparticles have become a subject of interest due to their enhanced activity and selectivity [1–3]. Particles formed on the surface of an inorganic or carbon support, however, have broad distribution in size and morphology [4,5] that lead to unstable catalytic properties [6,7]. A possible approach to overcome this problem is to grow the nanoparticles in structured polymers exhibiting well-defined interfaces [8,9]. Reports on nanoparticles formation in nanostructured polymeric media which show efficient catalytic properties have recently appeared [10,11].

In the present work we examine the incorporation of Ru(IV) in the matrix of hypercrosslinked polystyrene [12,13] and the formation and catalytic properties of the ruthenium nanoparticles developed therein. The test reaction, D-glucose oxidation, is of fundamental as well as technological interest [14]. Several methods based on chemical, electrochemical, biotechnological, and catalytic routes are currently available for the oxidation of D-glucose which serves as an intermediate in calcium gluconate synthesis [14]. The catalytic route promises to be the most viable. To increase the selectivity of oxidation, however, carbohydrate functional groups must be protected and the initial functional groups recovered after reaction, which results in a high loss of the target product [15,16]. The direct catalytic oxidation of D-glucose to D-gluconic acid, displayed in Fig. 1, allows one to avoid the protection stage. This reaction has been formerly performed in the presence of O_2 over noble metal catalysts deposited on activated carbon or aluminum oxide [7,17].

* Corresponding author.
E-mail addresses: sulman@online.tver.ru (E. Sulman), doludav@newmail.ru (V. Doluda).

1381-1169/$ – see front matter © 2007 Elsevier B.V. All rights reserved.
doi:10.1016/j.molcata.2007.08.029

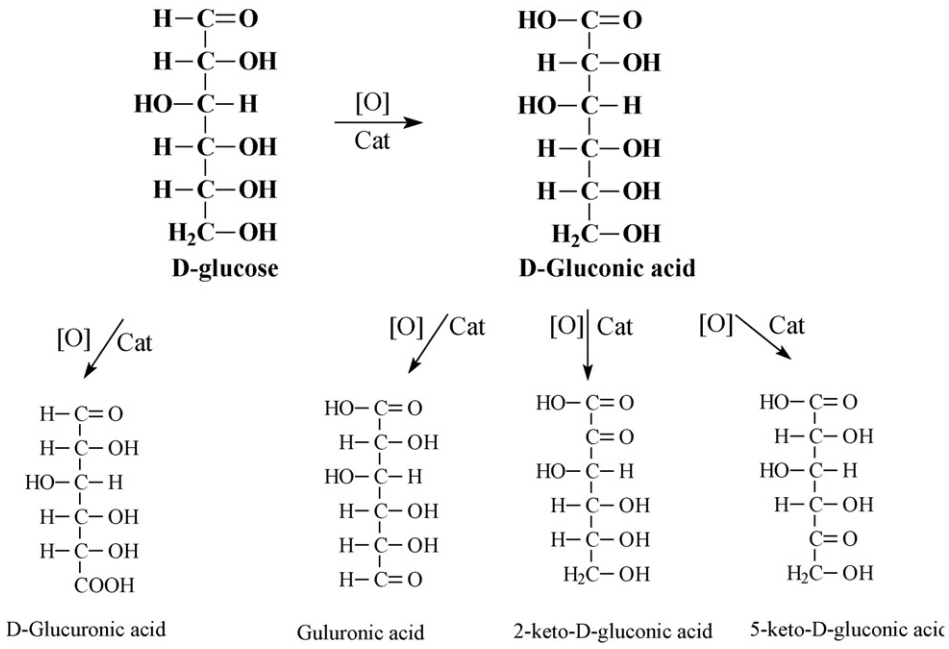

Fig. 1. Direct catalytic D-glucose oxidation and possible by-products.

It must be conducted in neutral or low-alkali media [18]. Selectivity may be increased through the addition of modifying agents at optimal loading levels [19], but the resultant selectivity unfortunately decreases at high rates of D-glucose conversion [20]. Therefore the synthesis of novel catalysts which display both high activity and selectivity is of special interest in this area.

2. Materials and methods

2.1. Materials

The hypercrosslinked polystyrene was purchased from Purolite Int. (UK), as Macronet MN 270/38600 type 2/100 (designated as MN-270). It was washed with acetone and water twice and purified under vacuum. Sodium hydrogen carbonate ($NaHCO_3$), sodium hydroxide (NaOH), hydrochloric acid (HCl) and ruthenium hydroxy chloride $Ru(OH)Cl_3$ were obtained from Reakhim (Moscow, Russia). Reagent-grade THF, methanol, hydrogen peroxide, gluconic acid and D-glucose were purchased from Aldrich and were used as received. Distilled water was purified with Elsi-Aqua water purification system.

2.2. Catalysts synthesis

In a typical synthesis, 0.24 g $Ru(OH)Cl_3$ was dissolved under air into 7 mL of a mixture of solvents consisting of 5 mL of THF, 1 mL of water and 1 mL of methanol, to which 3 g of MN-270 were added. The suspension was continuously stirred for 10 min so that the solution could be absorbed by the polymer, which was then dried at 75 °C for 1 h. The dried polymer matrix impregnated with $Ru(OH)Cl_3$ was boiled with 21 mL of 0.1 mol L^{-1} NaOH solution. Two milliliters of hydrogen peroxide were subsequently added to the suspension under continuous stirring. The catalyst was then recovered by filtration, washed with water at pH 6.4–7.0 and dried at 75 °C. Ru content was found to be 2.71 wt.% by XRF elemental analysis. Two other samples with different Ru weight contents (0.74 and 0.05%) were prepared following the same methodology.

2.3. D-Glucose oxidation methodology

The oxidation reaction was conducted batchwise in a PARR 4200 apparatus which provides independent control over parameters such as D-glucose and $NaHCO_3$ concentrations, catalyst concentration, temperature, (pure) oxygen feed rate, oxygen pressure and stirring rate. A suspension of the catalyst and an aqueous solution of D-glucose (20 mL) prepared at a predetermined concentration were placed in the reactor. The rate of oxygen feed was controlled by a rotameter. The equimolar quantity of the alkalizing agent ($NaHCO_3$) was fed to the apparatus continuously over 120 min (to maintain pH in the range 6.0–7.5), using an automatic dispenser. The high-stirring rates employed here ensured good mixing without diffusion limitation. Samples of the reaction mixture were periodically removed for analysis. At the end of each experiment, the catalyst was separated by filtration and the filtrate was analyzed to measure by HPLC the content in D-glucose and in the sodium salt of D-gluconic acid.

2.4. HPLC analysis

The analysis of the sodium salt of D-gluconic acid and D-glucose was performed using a MILLICHROM-4 HPLC chromatograph. Normal-phase chromatography using a 5 cm tungsten column characterized by a theoretical plate number of 4500 was chosen for sample analysis. Separon SGX-NH_2

(7 mkm) served as a stationary phase, whereas a 75/25 v/v acetonitrile/water solution was used as the mobile phase. The flow rate was held constant as 2 mL min^{-1} at 70 bar and 20 °C. The UV detector wavelength was maintained at 190 nm. The concentration of the sodium salt of D-gluconic acid and D-glucose varied from 0.001 to 10 mg mL^{-1} and the internal standard Xylite concentration was 1 mg mL^{-1}.

2.5. Determination of activation energies

The reaction was performed in an aqueous reaction medium, the catalyst concentration being 1.46×10^{-3} mol(Ru) L^{-1}, D-glucose concentration 2.78×10^{-2} mol L^{-1} and temperature varying from 25 to 80 °C. The apparent activation energy (E_a) was calculated according to the Arrhenius equation.

2.6. X-ray fluorescence analysis

Ru content was estimated by X-Ray fluorescence (XRF) measurements performed with a Spectroscan – Maks – GF1E spectrometer (Spectron, St-Petersburg, Russia) equipped with Mo anode, LiF crystal analyzer and SZ detector. The analyses were based on the Co Kα line and a series of HPS/Ru standards prepared by mixing 1 g of HPS with 10–20 mg of standard Ru compounds. The time of data acquisition (10 s) was constant.

2.7. Liquid nitrogen physisorption

Nitrogen physisorption was conducted at the normal boiling point of liquid nitrogen using a Becman Coulter SA 3100 apparatus (Coulter Corporation, Miami, Florida). Samples were degassed in a Becman Coulter SA-PREP apparatus for sample preparation (Coulter Corporation, Miami, Florida), at 120 °C in vacuum for 1 h, prior to the analysis.

2.8. TEM analysis

Transmission electron microscopy (TEM) experiments were performed on a 100 kV JEOL 100 CXII UHR microscope. After grinding of the sample, the powder was dispersed in pure ethanol. The suspension was stirred in an ultrasonic bath and one drop was placed on a carbon-coated copper grid.

2.9. X-ray absorption spectroscopy (XANES + EXAFS)

XAS measurements were carried out at HASYLAB (DESY in Hamburg, Germany) on the beamline X1 (Ru *K*-edge, 22117 eV) using a double-crystal Si(3 1 1) monochromator, which was detuned to 50% of maximum intensity to exclude higher harmonics in the X-ray beam. The spectra were recorded in the transmission mode at ambient temperature. The spectra were measured several times in order to check reproducibility. Reference spectra were recorded using standard reference compounds (RuO_2 and Ru-foil). Analysis of the EXAFS spectra was performed with the software VIPER for Windows [21].

Table 1
Surface areas and pore volumes for HPS-based catalysts before and after (*) 120 min of D-glucose oxidation

Catalyst	BET surface area ($m^2\ g^{-1}$)	Pore volume ($mL\ g^{-1}$)
HPS	1250	0.95
HPS–Ru-2.71%	1172	0.79
HPS–Ru-2.71%–OX*	1183	0.81
HPS–Ru-0.74%	1040	0.73
HPS–Ru-0.74%–OX*	1047	0.74
HPS–Ru-0.05%	1225	0.91
HPS–Ru-0.05%–OX*	1230	0.91

2.10. CO adsorption followed by diffuse reflectance infrared Fourier transform (DRIFT) spectroscopy

DRIFT spectra were recorded at ambient temperature with a Nicolet 460 Protégé spectrometer equipped with a diffuse reflectance attachment. The samples were placed in an ampoule supplied with a KBr window and 200 scans were collected from 400 to 6000 cm^{-1} with a 4 cm^{-1} resolution. CO adsorption was performed at ambient temperature at an equilibrium pressure of 20 Torr.

3. Results and discussions

3.1. Liquid nitrogen physisorption and X-ray fluorescence studies

BET surface areas and pore volumes of HPS and Ru-modified HPS are presented in Table 1. The values obtained for Ru-modified HPS are always lower than those for parent HPS; the introduction of Ru species in the HPS matrix leads to decrease of its BET surface area and pore volume. Changes after reaction are negligible (less than 1%).

Moreover, as shown in Fig. 2, the volume of mesopores with a pore mean diameter of 4 nm decreases when increasing of metal content, which suggests that ruthenium nanoparticles are local-

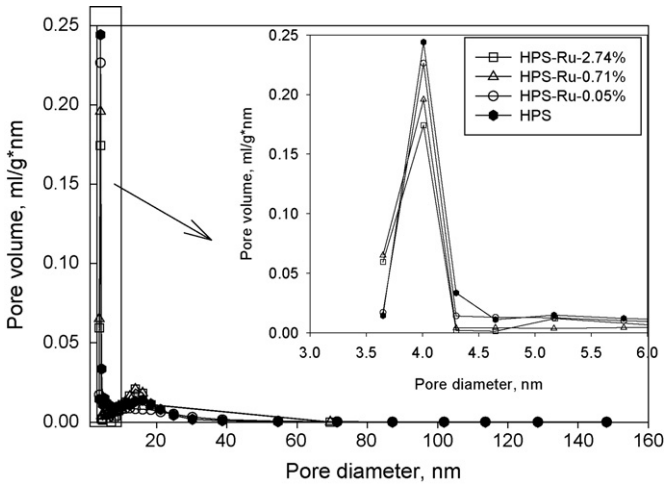

Fig. 2. Dependence of HPS and HPS-based catalysts pore volume vs. pore diameter.

Table 2
XFA analysis of HPS-based catalysts before and after (*) 120 min of D-glucose oxidation

Catalyst	Ru concentration (wt.%)
HPS–Ru-2.71%	2.71
HPS–Ru-2.71%–OX*	2.68
HPS–Ru-0.74%	0.74
HPS–Ru-0.74%–OX*	0.74
HPS–Ru-0.05%	0.05
HPS–Ru-0.05%–OX*	0.05

ized in these pores. The changes of pore volume for mesopores in the range of 5–25 nm, which can favor the transport of the reactants toward the active sites [11] are negligible for all catalyst samples. X-Ray fluorescence analysis shows that the decrease of Ru content in the three catalysts after D-glucose oxidation is negligible (Table 2). Leaching does not occur.

3.2. TEM studies

The porous nature of the polymer is evidenced in Fig. 3a, which shows a general view of sample HPS–Ru-0.74% after D-glucose oxidation. Nanoparticles can be seen on the three other micrographs (Fig. 3b–d), corresponding to each of the catalysts. Small nanoparticles (mean diameter 0.5–0.8 nm) coexist with less numerous larger ones (mean diameter up to 3.0 nm) or some aggregates. The presence of these clusters has been attributed to the hydrophobic nature of the polymer matrix which hinders to some extent a homogeneous distribution of the metal during its introduction in solution [11]. The overall mean diameter of nanoparticles in HPS–Ru-2.71% is measured to be 1.4 ± 1.2, while it is 1.0 ± 1.2 nm on the two other samples, less loaded in ruthenium and which do not contain particles larger than 2 nm.

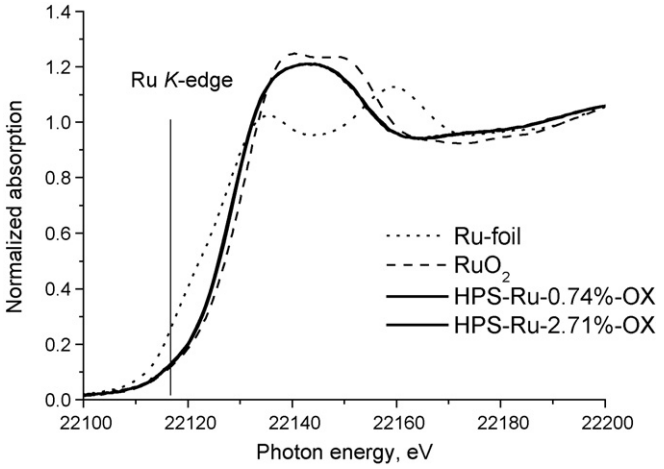

Fig. 4. XANES spectra of HPS–Ru samples and Ru reference compounds.

3.3. X-ray absorption spectroscopy

Fig. 4 shows the Ru K XANES spectra of Ru/HPS catalysts after 120 min of D-glucose oxidation and ruthenium references. In both Ru/HPS samples investigated, Ru electronic state is close to Ru^{4+}, indicating the oxidic nature of the nanoparticles (see in particular the position of the edge).

Indeed, Fourier transforms of the EXAFS signals (Fig. 5) confirm that the local environment around Ru is similar in both HSP–Ru-0.74%–OX and HPS–Ru-2.71%–OX samples. The intensity of the scattering events from the nearest and next-

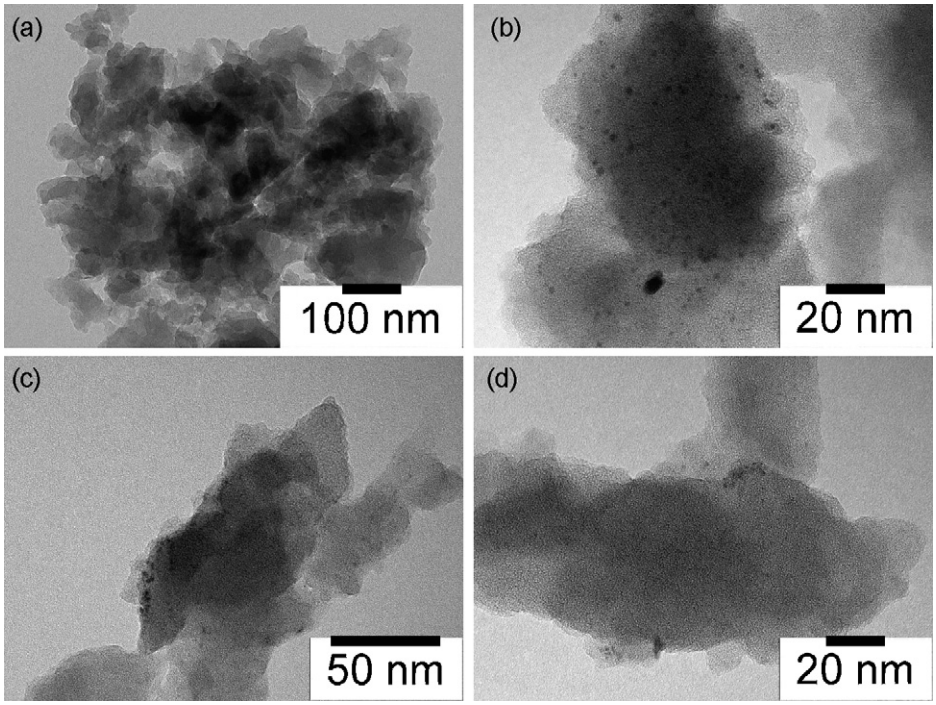

Fig. 3. TEM micrographs for (a) HPS–Ru-0.74%–OX (general view), (b) HPS–Ru-0.05%–OX, (c) HPS–Ru-0.74%–OX and (d) HPS–Ru-2.71%–OX after 120 min of D-glucose oxidation.

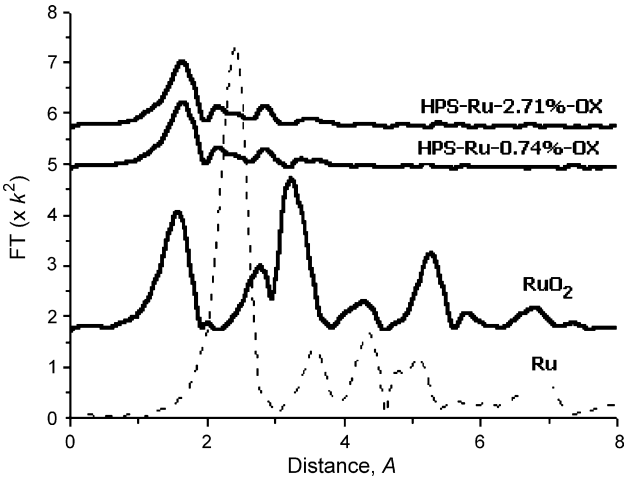

Fig. 5. FT transforms from the EXAFS signals of HPS–Ru samples and Ru reference compounds.

nearest neighbors is approximately the same. The first shell may be readily fitted in both (k and r) spaces with an average coordination number of 5.0 ± 0.1 atoms of oxygen located at 2.05–2.06 Å (with a Debye–Waller factor σ^2 of 6×10^{-3} Å^2).

The small shift towards lower photon energies compared with pure oxide, the decrease of the white line intensity (Fig. 5) and the presence of weak scattering events at distances close to those detected with Ru foil (Fig. 5) suggest though that Ru nanoparticles are not totally oxidic, and a metallic contribution may also be present.

3.4. CO adsorption DRIFT

Fig. 6 shows DRIFT CO spectra of ruthenium catalysts after 120 min of D-glucose oxidation. Infrared studies of CO sorption on ruthenium are not straightforward because Ru oxidation state tends to be modified in contact with CO, and stable multicarbonyl species which give rise to sets of two or three bands are formed. However, it has been reported that CO adsorption does not occur to a large extent on fully oxidized particles [22]. The detection of bands due to adsorbed CO thus lets us assume that nanoparticles in the pristine catalysts are not totally oxidic but also contain metallic species on the surface.

The spectrum recorded on HPS–Ru-2.71%–OX (Fig. 6a) exhibits two intense bands at 2002 and 2053 cm^{-1}, in the area attributed to stable dicarbonyl species on ionic ruthenium (usually considered to be Ru(II) [22]). Upon CO desorption, only the band at higher wavenumber remains. This can be interpreted as the presence of linear CO bonded on Ru^0 sites, which do not disappear upon decrease of the CO pressure, unlike dicarbonyls. The same bands are observed for HPS–Ru-0.74%–OX (Fig. 10b), accompanied by a weaker band at 2147 cm^{-1}. This band, considered along with a contribution from the central band, could be ascribed to dicarbonyl species formed upon Ru ions of oxidation state higher than (II) [22].

In this hypothesis, the mixed-valence nanoparticles supported on HPS–Ru-0.74%–OX, found by TEM to be slightly smaller than on HPS–Ru-2.71%–OX, and could be present in a more oxidized form than on the other sample. The band remaining after evacuation could be assigned to CO adsorption on the larger particles observed by TEM, which retain a larger metallic character than the smaller ones.

3.5. Influence of stirring rate on D-glucose oxidation

The stirring rate influence on D-glucose oxidation was investigated through a correlation between the global TOF calculated for a D-glucose conversion of 50% and the stirring rate, which was varied from 100 to 1000 rpm (Fig. 7). The catalyst concentration (C_c) was chosen as 0.0047 mol(Ru) L^{-1} and the substrate concentration (C_o) as 0.44 mol(Glu) L^{-1} for the three experiments. As it can be seen from Fig. 2, there are no mass transfer limitations above 800 rpm. In consequence, all further experiments were carried out at 1000 rpm.

3.6. Effect of catalyst and D-glucose concentration

The influence of the catalyst and D-glucose loading was examined by varying C_c from 0.0047 to 0.012 mol(Ru) L^{-1} and C_o from 0.44 to 1.11 mol(Glu) L^{-1}. The reaction temperature was 60 °C and the oxygen flow rate 0.018 m^3 h^{-1}. The reaction curves for the three catalysts are presented in Fig. 3 as a function of the substrate-to-catalyst ratio $q = C_o/C_c$. Decrease of q results in the appropriate increase of the reaction rate (Fig. 8a–c). These kinetic curves evidence the existence of a 10 min induction

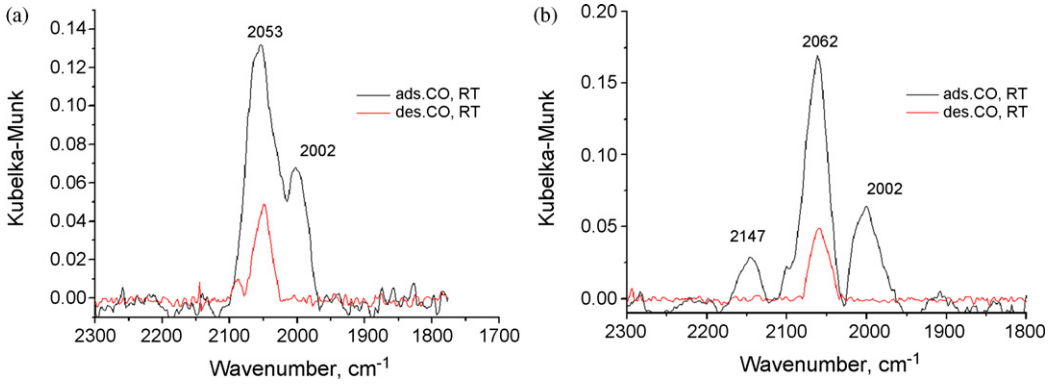

Fig. 6. DRIFT spectra of CO adsorbed on (a) HPS–Ru-2.71%–OX and (b) HPS–Ru-0.74%–OX.

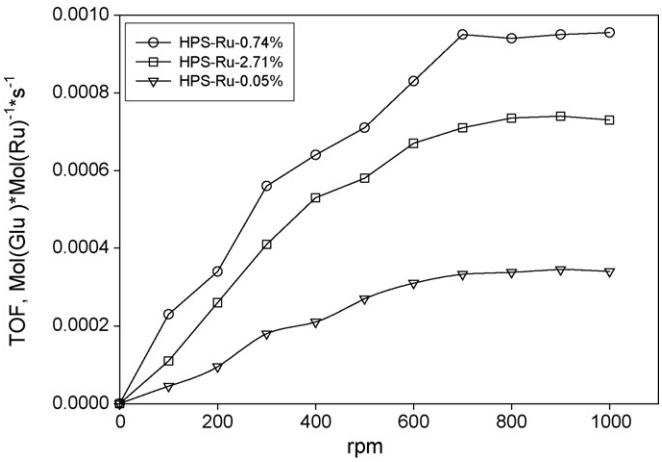

Fig. 7. Dependence of TOF vs. stirring rate for HPS-based catalysts.

period with negligible D-glucose conversion, as was observed for L-sorbose oxidation on Pt HPS-based catalysts [11]. It can be seen from Fig. 3d that there is a strong correlation between selectivity to D-gluconic acid and substrate-to-catalyst ratios q. The decrease of the ratio q leads to a substantial increase of the selectivity towards the formation of D-gluconic acid.

The highest TOF and selectivity were determined for HPS–Ru 0.74% at a catalyst concentration of 0.012 mol(Ru) L^{-1} and a D-glucose concentration of 0.44 mol(Glu) L^{-1} (ratio $q = 37.4$) (Table 3). All further experiments were carried out in these conditions in order to reach maximum TOF and selectiv-

Table 3
Kinetic measurements for HPS-based catalysts

Catalyst	TOF (mol mol Ru^{-1} s^{-1})[a]	Conversion (%)	Selectivity (%)
HPS–Ru 2.71%	1.03×10^{-3}	95.3	99.3
HPS–Ru 0.74%	1.13×10^{-3}	99.4	99.8
HPS–Ru 0.05%	0.76×10^{-3}	80.3	98.6

[a] TOF $= C(\text{Glu})\alpha/(C(\text{Ru})t \times 100)$, where α is the conversion (%) and t is the time (s).

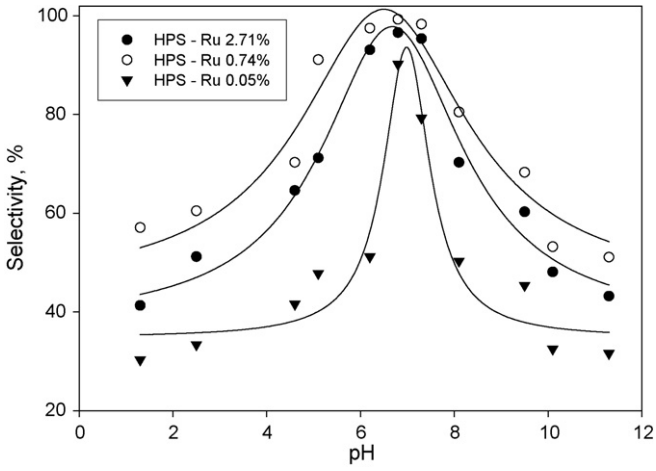

Fig. 9. Dependence of selectivity on pH.

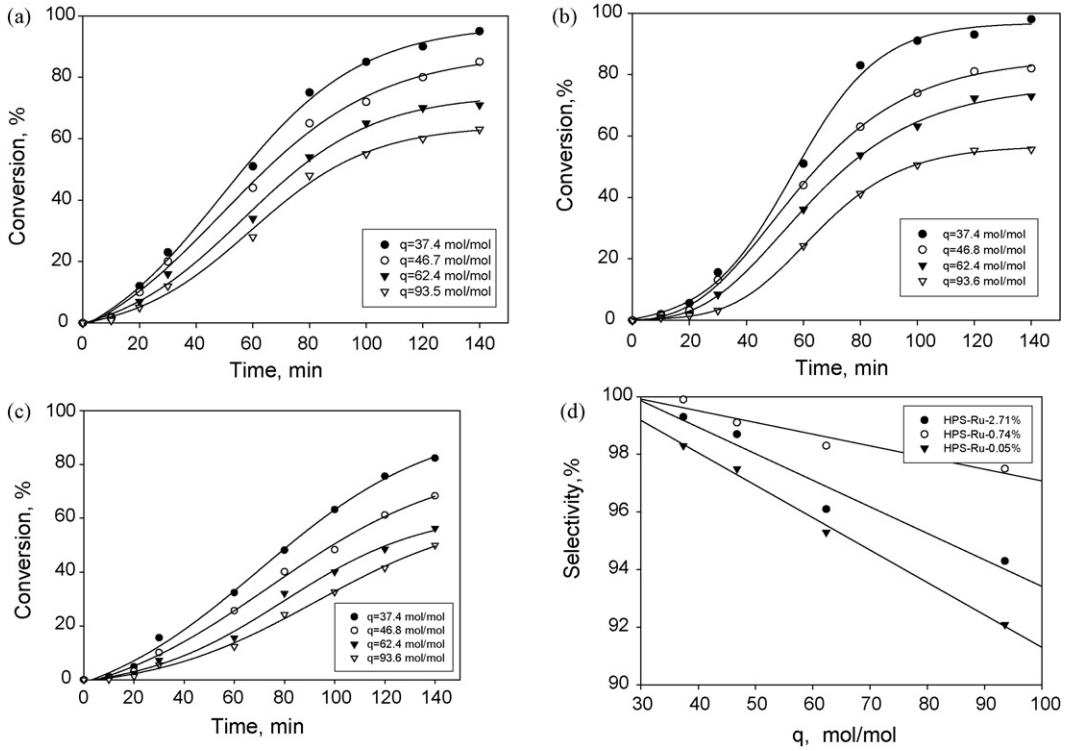

Fig. 8. Dependence of D-glucose conversion vs. time on different catalysts: (a) HPS–Ru-2.71%, (b) HPS–Ru-0.74%, (c) HPS–Ru-0.05% and (d) dependence of selectivity toward D-gluconic acid formation for various substrate-to-catalyst ratios q and a conversion of 90%.

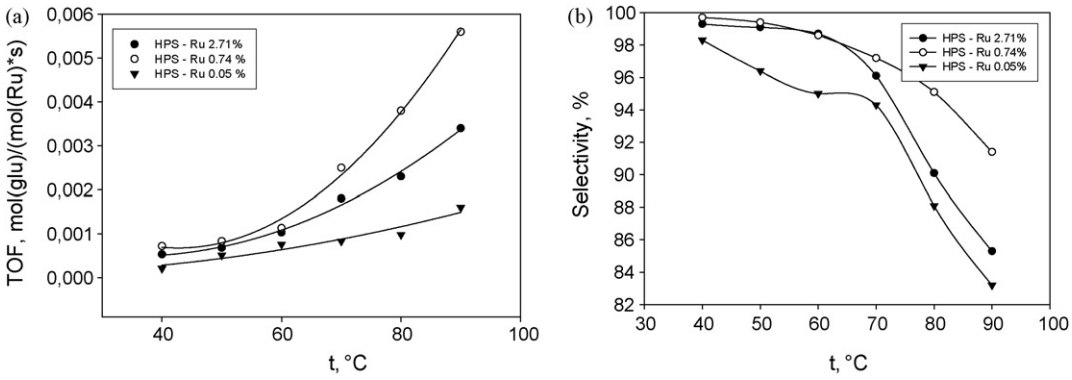

Fig. 10. (a) Dependence of HPS-based catalysts activity on the reaction temperature and (b) dependence of selectivity toward D-gluconic acid formation on the reaction temperature.

ity. HPS–Ru 2.71% and HPS–Ru-0.05% exhibit lower turnover frequencies and selectivities than HPS–Ru 0.74%.

3.7. Effect of pH

In order to investigate the pH influence on activity and selectivity of D-glucose oxidation, the process was carried out at pH ranging from 1.4 to 11. NaOH and HCl solutions were used to reach extreme pH. Fig. 9 shows the effect of pH on the selectivity of D-glucose oxidation to D-gluconic acid at 80% conversion. Maximum selectivity is observed when the reaction is performed at pH 6.5–7.2, in line with earlier report [18]. At pH lower than 6 and higher than 8, selectivity strongly diminishes. The pH range giving optimum selectivity was used in all the experiments. More abrupt changes of selectivity and activity with pH change are observed for HPS-Ru 0.05% sample.

3.8. Effect of reaction temperature

Fig. 10a shows that the reaction temperature has a strong positive effect on the activity of nanostructured catalysts, especially HPS–Ru 0.74%. The selectivity of D-glucose oxidation to D-gluconic acid between 30 and 60 °C remains close to 97–99% on HPS–Ru 2.71% and HPS–Ru 0.74% but slightly decreases from 98 to 95% on HPS–Ru 0.05% (Fig. 10b). With a further rise of temperature, the selectivity decreases strongly up to about 85% for HPS–Ru 2.71% and HPS–Ru 0.05%, but only to 92% for HPS–Ru 0.74%. It means that selectivity of D-glucose oxidation to D-gluconic acid is more stable on HPS–Ru 0.74% with respect to reaction temperature.

3.9. Activation energy of the reaction

To get an insight into the effect of polymer matrix and metal loading on D-glucose oxidation, the activation energy of the reaction was determined. The values of apparent activation energy (E_a) and preexponentional factor (k_0) estimated for the three catalysts are given in Table 4. E_a are very close for all the catalysts; values of 35–41 kJ mol^{-1} were also measured on Pt HPS-based catalysts for L-sorbose oxidation [10,11]. It suggests that similar active sites are present on the three samples. However, the highest k_0 value obtained on HPS–Ru 0.74% lets one assume that this sample exhibits the highest quantity of active sites.

Table 4
Activation energy and preexponential factor for HPS-based catalysts

Catalyst	E_a (kJ mol^{-1})	k_0
HPS–Ru-2.71%	39	9.6×10^4
HPS–Ru-0.74%	42	19.2×10^4
HPS–Ru-0.05%	37	7.13×10^4

4. Conclusions

Ru-containing hypercrosslinked polystyrene systems with different loadings of metal are described in this paper. The formation of nanoparticles seems to be restricted by the size of HPS nanocavities, limiting the size of the particles around a mean diameter of 1.0–1.4 nm. The nanoparticles seem to have a mixed valence structure, with both oxidic and metallic components. No leaching of the active phase is noted during the reaction. Catalytic activities and selectivities of the catalysts towards the oxidation of D-glucose into D-gluconic acid have been measured under a wide variety of reaction conditions. The most active catalyst was found to contain 0.74 Ru wt.%. The highest selectivity of D-glucose oxidation measured on this system was 99.8% at 99% D-glucose conversion and the activity of the catalyst calculated as 1.13×10^{-3} mol mol^{-1} Ru s^{-1}. The synthesized catalysts have higher activity and selectivity compare to common used carbon based catalyst [19,20]. The high catalytic activity is attributed to the presence of pores of different sizes, which facilitate mass transport and the high stability is attributed to the presence of small mesopores that have high sorptional capacity and prevent the leaching of the active phase.

Acknowledgement

This work has been supported by the 6th Framework Program project “NANOCAT” (contract number 506621-1).

References

[1] R. Brayner, G. Viau, F. Bozon-Verduraz, J. Mol. Catal. A: Chem. 182/183 (2002) 227–238.
[2] C. Liu, Y. Xu, S. Liao, D. Yu, J. Mol. Catal. A: Chem. 157 (2000) 253–259.
[3] A. Drelinkiewicz, M. Hasik, M. Kloc, J. Catal. 186 (1999) 123–133.
[4] K. Okitsu, A. Yue, S. Tanabe, H. Matsumoto, Chem. Mater. 12 (2000) 3006–3011.
[5] A. Horvath, A. Beck, A. Sarkany, L. Guczi, Solid State Ionics 148 (2002) 219–225.
[6] A. Abbadi, M. Makkee, W. Visscher, J.A.R. Vanveen, H. Vanbekkum, J. Carbohydr. Chem. 12 (1993) 573.
[7] J.J. Ostermaier, J.R. Katzer, W.H. Manoque, J. Catal. 41 (1976) 277–292.
[8] C. Sanchez, G.J. Soler-Illia, F. Ribot, T. Lalot, C.R. Mayer, V. Cabuil, Chem. Mater. 13 (2001) 3061–3083.
[9] V. Sankaran, C.C. Cummins, R.R. Schrock, R.E. Cohen, R.J. Silbey, J. Am. Chem. Soc. 112 (1990) 6858–6859.
[10] S.N. Sidorov, I.V. Volkov, V.A. Davankov, M.P. Tsyurupa, P.M. Valetsky, L.M. Bronstein, R. Karlinsey, J.W. Zwanziger, V.G. Matveeva, E.M. Sulman, N.V. Lakina, E.A. Wilder, R.J. Spontak, J. Am. Chem. Soc. 123 (2001) 10502–10510.
[11] L.M. Bronstein, G. Goerigk, M. Kostylev, M. Pink, I.A. Khotina, P.M. Valetsky, V.G. Matveeva, E.M. Sulman, M.G. Sulman, A.V. Bykov, N.V. Lakina, R.J. Spontak, J. Phys. Chem. B 108 (2004) 18234–18242.
[12] V.A. Davankov, M.P. Tsyurupa, React. Polym. 13 (1990) 27–42.
[13] M.P. Tsyurupa, V.A. Davankov, J. Polym. Sci.: Polym. Chem. Ed. 18 (1980) 1399–1406.
[14] K.B. Kokoh, J.M. Leger, B. Beden, C. Lamy, Electrochim. Acta 37 (1992) 1333–1342.
[15] H.A. Lyazidi, M.Z. Benabdallah, J. Berlan, C. Kot, P.L. Fabre, M. Mestre, J.F. Fauvarque, Can. J. Chem. Eng. 74 (1996) 405–411.
[16] P. Cognet, J. Berlan, G. Lacoste, P.L. Fabre, J.M. Jud, J. Appl. Electrochem. 25 (1995) 1105–1112.
[17] M. Wenkin, C. Renard, P. Ruiz, B. Delmon, M. Devillers, Stud. Surf. Sci. Catal. 108 (1997) 391–398.
[18] J.M.H. Dirkx, H.S. van der Baan, J. Catal. 67 (1981) 1–13.
[19] M. Wenkin, C. Renard, P. Ruiz, B. Delmon, M. Devillers, Stud. Surf. Sci. Catal. 110 (1997) 517–526.
[20] M. Wenkin, P. Ruiz, B. Delmon, M. Devillers, J. Mol. Catal. A: Chem. 180 (2002) 141–159.
[21] K.V. Klementiev, VIPER for Windows (Visual Processing in EXAFS Researches), Freeware. http://www.desy.de/∼klmn/viper.html.
[22] K.I. Hadjiivanov, G.N. Vayssilov, Adv. Catal. 47 (2002) 307–511.